

Tetragonal and trigonal deformations in zinc-blende semiconductors: A tight-binding point of view

J.-M. Jancu and P. Voisin

Laboratoire de Photonique et de Nanostructure, CNRS, route de Nozay, F-91000 Marcoussis, France

(Received 9 January 2007; revised manuscript received 21 July 2007; published 18 September 2007)

The deformation potentials of cubic semiconductors are reexamined from the point of view of the extended-basis $sp^3d^5s^*$ tight-binding model. Previous parametrizations had failed to account properly for trigonal deformations, even leading to incorrect sign of the acoustic component of the shear deformation potential d . The strain-induced shifts and splittings of the on-site energies of the p and d orbitals are shown to play a prominent role in obtaining satisfactory values of deformation potentials both at the zone center and zone extrema. The present approach results in excellent agreement with available experimental data and recent *ab initio* calculations.

DOI: [10.1103/PhysRevB.76.115202](https://doi.org/10.1103/PhysRevB.76.115202)

PACS number(s): 71.15.Ap, 71.55.Eq, 73.21.La, 85.75.-d

The effect of uniaxial stress on the band structure of semiconductors has been a major theoretical and experimental topic for many years. With the development of strained-layer epitaxy, it has also become an important issue in modern material science and device physics. In their seminal approach, nearly half a century ago, Bir and Pikus established the strain Hamiltonian using the theory of invariants.¹ It depends on a number of deformation potentials describing the shifts and splittings of the various band extrema. For instance, for a given band near the Brillouin zone center, it reads as

$$H_\epsilon^i = -a^i(\epsilon_{xx} + \epsilon_{yy} + \epsilon_{zz}) - 3b^i \left[\left(L_z^2 - \frac{1}{3} \mathbf{L}^2 \right) \epsilon_{zz} + \text{cp} \right] - \frac{6}{\sqrt{3}} d^i (\{L_x L_y\} \epsilon_{xy} + \text{cp}), \quad (1)$$

where ϵ_{ij} are the components of the strain tensor ϵ , \mathbf{L} is the angular momentum operator, $\{L_x L_y\} = \frac{1}{2}(L_y L_x + L_x L_y)$, and cp refers to circular permutations with respect to the axes x , y , and z . The coefficient a^i is the hydrostatic deformation potential for the i th band, while b^i and d^i are, respectively, the tetragonal and rhombohedral (or trigonal) deformation potentials. We now explicit Eq. (1) for the Γ_6 and Γ_8 states of zinc-blende crystals: the Γ_6 conduction-band energy only depends on the hydrostatic term owing to the $L=0$ matrix representation of the momentum operator. For the Γ_8 valence-band edge, the heavy- and light-hole degeneracy is lifted (as $L=1$) and the splitting depends on the strain orientation. Under [001] uniaxial stress or for lattice mismatched epilayers grown along the [001] direction, strain components can be written as $\epsilon_{xx} = \epsilon_{yy} \neq \epsilon_{zz}$ and $\epsilon_{xy} = \epsilon_{yz} = \epsilon_{zx} = 0$. Thus, the heavy- and light-hole bands split by an amount proportional to b . Under [111] stress or for mismatched epilayers grown along the [111] direction, we have $\epsilon_{xx} = \epsilon_{yy} = \epsilon_{zz} \neq 0$ and $\epsilon_{xy} = \epsilon_{yz} = \epsilon_{zx} \neq 0$, giving a valence-band splitting proportional to d . The two situations also differ by the presence or not of a static displacement of the anion and cation sublattices: in the former case, all the atomic bonds in the strained crystal retain the same length and same angle with respect to the strain symmetry axis, giving no short range contribution to the

strain Hamiltonian. Conversely, for trigonal distortions, the equilibrium positions of atoms are no longer fully determined by stress invariants and a relative displacement of the sublattices is allowed. The resulting internal strain is represented by the Kleinmann parameter ζ , which ranges between 0 and 1.² The value $\zeta=1$ corresponds to a deformation with the same symmetry as the [111] strain but maintaining equal bond lengths of $a_0\sqrt{3}/4$, whereas $\zeta=0$ is related to the macroscopic strain that does not account for sublattice displacement. This gives simultaneously a long range or acoustic (d') and a short range or optical (d_0) contribution to the rhombohedral deformation potential d ,³

$$d = d' - \frac{\zeta}{4} d_0. \quad (2)$$

The strain Hamiltonian has been extensively used in connection with the $\mathbf{k} \cdot \mathbf{p}$ theory to interpret experimental data and measure parameters. On a more fundamental side, several *ab initio* calculations of the deformation potentials have been reported. More recently, atomistic approaches using empirical parameters have become a strong challenge to the $\mathbf{k} \cdot \mathbf{p}$ theory for a precise modeling of semiconductor nanostructures, where compositions and deformations can vary rapidly at the bond-length scale. A remarkable feature of atomistic theories (as opposed to the fundamentally perturbative character of the $\mathbf{k} \cdot \mathbf{p}$ theory) is their natural ability to treat the whole Brillouin zone. It follows that a “good” atomistic model must give a proper account of general distortions not only in the vicinity of the fundamental gap but also at the edges of the Brillouin zone: the effects of strain actually are a very stringent test of atomistic models. Here, we examine the effects of tetragonal and trigonal deformations from the point of view of the empirical tight-binding (TB) theory.

Within the tight-binding formalism, strain effects are mainly determined by scaling the Slater-Koster two-center integrals⁴ (or transfer integrals) with respect to bond-length alterations, while bond-angle distortions are automatically incorporated via the phase factors in the Slater-Koster matrix elements. This leaves a more than sufficient number of strain-dependent parameters to fit the deformation potentials at the Brillouin zone center. However, when trying to fit

simultaneously the splitting of zone-edge conduction valleys, one encounters a difficulty. For the case of [001] uniaxial strain, it was shown in Ref. 7 that adding a term corresponding to a strain-induced splitting of the d orbital on-site energies (one-center integrals) leads to a much better overall fit of the deformation potentials at Γ and X . Indeed, since the Wannier functions of tight-binding models are Slater-type orbitals,⁵ the one-center integrals are expected to be sensitive to the environment of neighboring atoms. In principle, one should also introduce a [001] shear parameter of the on-site p energies, and this can be generalized to all diagonal matrix elements in proportion to hydrostatic and uniaxial distortions.⁶ However, in the atomic limit, the on-site properties should depend neither on strain nor on chemical environment. This is nearly the case for the s and p valence states that display an excellent degree of transferability. Conversely, it is clear that the excited s^* and d -like orbitals have a strong free-electron character and corresponding energies must depend on strain-induced effects. Finally, one should remember that the “rule of the game” of atomistic models is to limit the number of empirical parameters to the minimum required to account for symmetries and reproduce experimental (or *ab initio*) band parameters within a given accuracy. For instance, the hydrostatic shifts of on-site energies appeared to be useless parameters at the present level of model sophistication, as they are for a large part renormalized in the variation of transfer integrals with bond-length changes.

To the best of our knowledge, the case of trigonal deformations has never been discussed in the framework of an advanced tight-binding model. The first difficulty is the choice of a value for the internal-strain parameter ζ : contrarily to *ab initio* calculations, the atomic positions are an input of the tight-binding model, not a result of the calculation. ζ can be obtained theoretically either in *ab initio* calculations or from the fit of phonon dispersions, as first demonstrated by Nielsen and Martin.⁸ ζ was precisely measured by x-ray diffraction for Si and Ge. The common value $\zeta=0.54$ (Ref. 9) is in agreement with first-principles calculations.⁸ However, for GaAs, the most-cited experimental result $\zeta=0.76$ (Ref. 13) is still controversial^{8,10,14,15} and differs significantly from the theoretical value $\zeta=0.48$ obtained by Nielsen and Martin.⁸ Note that the latter value gives an excellent representation of elastic constants and phonon frequencies of GaAs and is corroborated by recent x-ray measurements, which give $\zeta=0.55$.¹⁰ The second difficulty is methodological since a fit of d comes out of a calculation, while there are two quantities to determine, d' and d_0 . Here, d' is obtained by running the code using the fit parameters and setting $\zeta=0$, whereas a relative displacement of the anion and cation sublattices in the absence of macroscopic strain is used to calculate d_0 .

The need for introducing a new shear parameter is evidenced by the failure of simpler tight-binding models: in the minimal sp^3 basis, the TB Hamiltonian cannot describe both b and d satisfactorily, as seen for the diamond structure where b , d' , and d_0 are linked by the analytical relations³

$$d_0 = 16d' = -\frac{16}{\sqrt{3}}b. \quad (3)$$

For Ge, fitting $b=-1.88$ eV \pm 0.12 (Ref. 11) and considering $\zeta=0.54$, one obtains $d=-1.26$ eV, in poor agreement with the experimental result, $d=-5.0\pm 0.5$ eV.¹² The failure is mainly caused by an erroneous positive deformation potential d' [see Eq. (3)] in sharp contrast with the sign calculated by the self-consistent linear muffin-tin orbital (LMTO) and *ab initio* pseudopotential approaches,^{14,15} which show a strong redistribution of the valence-electron density induced by the acoustic deformation. Similar discrepancies are obtained numerically for the zinc-blende semiconductors and no significant changes appear within the $sp^3s^*d^5$ approach, until a splitting of on-site energies is introduced. The corresponding Hamiltonian obviously depends on the strain direction. For a uniaxial stress along [001], the perturbation has the Γ_{12} symmetry, and the crystal field splits the fivefold degenerate d orbitals into two doublets and a singlet as

$$\begin{aligned} E_{d_{xz}} = E_{d_{yz}} &= E_d[1 - \delta_{001}(\epsilon_{zz} - \epsilon_{xx})], \\ E_{d_{x^2-y^2}} &= E_{d_{3z^2-r^2}} = E_d, \\ E_{d_{xy}} &= E_d[1 + 2\delta_{001}(\epsilon_{zz} - \epsilon_{xx})]. \end{aligned} \quad (4)$$

For a uniaxial strain along [111], the perturbation has the Γ_{15} symmetry and also splits the five equivalent d bands into two doublets and a singlet state. To handle this case, it is more convenient to rotate the coordinate system and choose the quantization axis \bar{z} along the [111] direction. To avoid confusions, we name “(111) basis” the new $(\bar{x}, \bar{y}, \bar{z})$ basis.

The on-site d energies now corresponds to the representations A_1 with $E_{d_{3\bar{z}^2-r^2}}$, E_1 with $E_{d_{\bar{x}\bar{z}}}$ and $E_{d_{\bar{y}\bar{z}}}$, and E_2 with $E_{d_{\bar{x}^2-\bar{y}^2}}$ and $E_{d_{\bar{x}\bar{y}}}$,

$$\begin{aligned} E_{d_{3\bar{z}^2-r^2}} &= E_d[1 - 2\delta_{111}(\epsilon_{\bar{z}} - \epsilon_{\bar{x}})], \\ E_{d_{\bar{x}\bar{z}}} = E_{d_{\bar{y}\bar{z}}} &= E_d[1 + \delta_{111}(\epsilon_{\bar{z}} - \epsilon_{\bar{x}})], \\ E_{d_{\bar{x}^2-\bar{y}^2}} &= E_{d_{\bar{x}\bar{y}}} = E_d, \\ \epsilon_{\bar{z}} - \epsilon_{\bar{x}} &= \frac{8}{3}(1 - \zeta)\epsilon_{xy}. \end{aligned} \quad (5)$$

Negative ϵ_{xy} corresponds to conventional compressive stress. δ_{001} and δ_{111} are shear parameters fitted to reproduce the tetragonal and the trigonal deformation of the valence-band edge, respectively. Note that, since perturbations result from different modifications of the nearest neighbor positions, there is no reason for an exact geometrical relation linking δ_{001} (Ref. 16) and δ_{111} . The scheme of level splittings for uniaxial compressions along [001] and [111] is shown in Fig. 1. Following this procedure, we demonstrate excellent agreement with experiment for b and d . In addition, the figures coming out for the acoustic deformation potential d' are consistent with self-consistent LMTO results.¹⁴ For instance, for Ge, using the parametrization of Ref. 7, with $\delta_{001}=0.54$

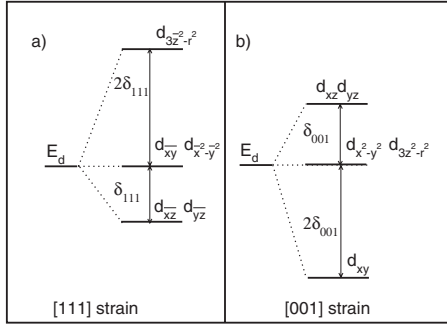


FIG. 1. Schematic plot of energy-level splitting of d states induced by a uniaxial strain along the [111] (left panel) and [001] directions (right panel). For [111] strain, the quantization axis \bar{z} is chosen along the [111] direction.

and $\delta_{111} = +1.5$, we get $b = -1.9$ eV, $d = -4.6$ eV, and $d' = -1.37$ eV, in agreement with experiment, $b = -1.88 \pm 0.12$ eV¹¹ and $d = -5.0$ eV ± 0.5 ,¹² and the LMTO calculation, $d' = -1.3$ eV.¹⁴ Noteworthy, the fit values of δ_{001} and δ_{111} are comparable to their purely geometrical counterpart in the free-electron case, 0.75 and 2, respectively. These results indicate that this simple approach is sufficient to properly account for general $[klm]$ strains in semiconductor nanostructures at the Γ point.

As discussed in Ref. 7, introduction of δ_{001} allows to obtain simultaneously a fit of b and of the conduction-band splitting of X valleys under [001] stress. However, for [111] stress, when examining the shear deformation potential of the L_1 conduction extrema, using our fit value of δ_{111} , we find a large and disappointing discrepancy: we obtain $D_1^{5c} = 7.5$ eV, to be compared with the experimental value of 16.6 ± 0.4 eV measured from optical absorption near the direct and indirect gaps by Balslev.¹⁷ Note that the large experimental value was obtained by several independent measurements.¹⁷ However, this value is in contradiction with recent density-functional results in the local-density approximation¹⁸ converging toward $D_1^{5c} = 11.3$ eV. In the absence of recent experimental data, it is difficult to resolve this contradiction. In the following, we examine the parametrization flexibility of the $spds$ TB model in the calculation of shear deformation potential at L . From a quantum chemistry point of view, the discrepancy for D_1^{5c} could be understood from the fact that the L conduction band minimum is dominated by s and p states, in contrast with wave functions at X that have a strong d character.⁷ Therefore, the inclusion

of splitting of on-site p energies might be necessary for a reliable description of strain field anisotropies at the L point. This is also compatible with a free-electron description of TB parameters,⁷ where splittings of degenerate p and d orbitals occur for the empty crystal under uniaxial stress. At this point, the internal logic of the model implies that if the strain-induced splittings of the one-center integrals play such an important role, their shift under hydrostatic strain should also be taken explicitly into account instead of being renormalized in a strain dependency of two-center integrals. Using again the (111) basis, the corresponding contributions to (111)-strain Hamiltonian are written as

$$E_{p_{\bar{x}}} = E_{p_{\bar{y}}} = E_p [1 + \pi_{111}(\epsilon_{\bar{z}} - \epsilon_{\bar{x}})],$$

$$E_{p_{\bar{z}}} = E_p [1 - 2\pi_{111}(\epsilon_{\bar{z}} - \epsilon_{\bar{x}})]. \quad (6)$$

To achieve a complete description of strain effects in the $spds^*$ model, on-site Hamiltonian matrix elements E_i were also scaled with respect to bond-length changes,

$$E_i(l) = E_i(l_0) \left(\frac{l_0}{l} \right)^{n_i}, \quad (7)$$

where l (l_0) is the strained (unstrained) interatomic distance and n_i are the orbital-dependent exponents. The TB parameters and scaling constants for Ge are listed in Table I. They were derived from the original $sp^3s^*d^5$ parameter system⁷ and optimized to fulfill the requirement of very good agreement with recent *ab initio* calculations and experimental band parameters. The target values are the critical-point energies of valence and conduction bands, spin-orbit splitting, the measured electron and hole effective masses, pressure coefficients of band gaps, and LDA-corrected deformation potentials of valence and conduction states. We found that the dependence of energy bands on strain effects is correctly reproduced using the most plausible value $D_1^{5c} = 11.3$ eV. Although the number of tight-binding parameters is increased with respect to Ref. 7, their numerical determination through a multiparameter fitting procedure still converges very well and resulting values gain a more intuitive view of chemical dependencies. In particular, for the high-lying states d and s^* , the corresponding exponents, n_{s^*} , n_d , $n_{s^*s^*}$, n_{s^*d} , n_{dd} , $n_{dd\pi}$, and $n_{dd\delta}$, are of the order of 2, which guarantee that the high-energy parts of the band structure scale as the free-electron l^{-2} distance law. Conversely, the interactions within the subset $\{s, p\}$ are expected to reflect the localization of the

TABLE I. Tight-binding parameters (in eV) and dimensionless scaling constants for Ge. The energy zero is taken at the valence-band maximum.

E_s	-3.4407	$ss\sigma$	-1.5319	$sp\sigma$	2.7737	n_s	0.2983	$n_{ss\sigma}$	3.7821	$n_{sp\sigma}$	0.7086
E_p	4.1342	$s^*s^*\sigma$	-3.5836	$s^*p\sigma$	2.0249	n_p	0.8687	$n_{s^*s^*\sigma}$	2.000	$n_{s^*p\sigma}$	1.8932
E_d	13.2395	$s^*s\sigma$	-1.9099	$sd\sigma$	-3.1063	n_d	1.9321	$n_{s^*s\sigma}$	0.0	$n_{sd\sigma}$	1.2
E_s^*	19.1761	$pp\sigma$	4.0981	$s^*d\sigma$	-0.8989	n_{s^*}	2.00	$n_{pp\sigma}$	2.2079	$n_{s^*d\sigma}$	2.0
$\Delta/3$	0.1275	$pp\pi$	-1.5223	$dd\delta$	-2.1389	$n_{pp\pi}$	0.8741	$n_{dd\delta}$	2.4515	π_{111}	0.1938
		$pd\sigma$	-1.8229	$dd\sigma$	-1.2172	$n_{pd\sigma}$	1.2817	$n_{dd\sigma}$	2.5458	δ_{001}	0.6502
		$pd\pi$	1.9001	$dd\pi$	2.5054	$n_{pd\pi}$	1.5435	$n_{dd\pi}$	2.3556	δ_{111}	0.7897

TABLE II. Comparison of uniaxial and hydrostatic deformation potentials obtained in the present work with *ab initio* and experimental results for Ge.

	b	d_0	d'	d	D_1^{5c}	a_v	a_c
This work	-1.87	22.6	-1.5	-4.8	11.5	2.1	-7.9
<i>Ab initio</i>		22.4 ^a	-1.3 ^a	-5.0 ^a	11.3 ^b , 17.8 ^c	2.23 ^d	-7.83 ^d
Expt.	-1.88 ^e	33 ^f		-5.0 ^f	18.4 ^f		

^aReference 14.^bReference 18.^cReference 20.^dReference 19.^eReference 11.^fReference 12.

atomic wave functions s and p near the nuclei and the scaling constants n_s , n_p , $n_{ss\sigma}$, $n_{sp\sigma}$, $n_{pp\sigma}$ and $n_{pp\pi}$ should differ from the free-electron value. This is observed in our results that also give the correct trends for the valence bands, $n_{pp\sigma} \gg n_{pp\pi}$, not reproduced in the previous parametrization.⁷ The data presented in Table II demonstrate that our results are in good agreement with experimental and theoretical values for d and D_1^{5c} . The magnitude and sign of d' and d_0 are well reproduced compared to the LMTO calculations. The present value for d_0 differs from the experimental results whose values are actually controversial, a discrepancy observed already earlier (compare Table I). We note finally that our results also agree with recent *ab initio* calculations¹⁹ for the hydrostatic deformation potentials of the Γ_{8v}^+ valence-band maximum (a_v) and Γ_{7c}^- conduction-band minimum (a_c).

In conclusion, we have demonstrated that the $sp^3d^5s^*$ model requires diagonal matrix element shifts to correctly reproduce uniaxial $[klm]$ strain for cubic semiconductors. In order to test our model, we have calculated the acoustic and optical contributions to the trigonal deformation potentials and found good agreement with experiment and LMTO results. A major improvement compared to smaller TB models was the correct sign and magnitude of the acoustic deformation potential d' directly related to the shear parameter of d states. This TB model provides a valid framework for the calculation of strain effects in self-assembled quantum dots.

The authors thank L. Pedesseau for unpublished LDA calculations and F. Glas for clarifying discussions.

¹G. L. Bir and G. E. Pikus, *Symmetry and Strain-Induced Effects in Semiconductors* (Wiley, New York, 1974).

²L. Kleinmann, Phys. Rev. **128**, 2614 (1962).

³A. Blacha, H. Presting, and M. Cardona, Phys. Status Solidi B **126**, 11 (1984).

⁴J. C. Slater and G. F. Koster, Phys. Rev. **94**, 1498 (1954).

⁵W. Kohn, Phys. Rev. B **10**, 4388 (1973).

⁶T. B. Boykin, G. Klimeck, R. C. Bowen, and F. Oyafuso, Phys. Rev. B **66**, 125207 (2002).

⁷J.-M. Jancu, R. Scholz, F. Beltram, and F. Bassani, Phys. Rev. B **57**, 6493 (1998).

⁸O. H. Nielsen and R. M. Martin, Phys. Rev. Lett. **50**, 697 (1983); Phys. Rev. B **32**, 3792 (1985); O. H. Nielsen, *ibid.* **34**, 5808 (1986).

⁹C. S. G. Cousins, L. Gerward, J. Staun Olsen, B. Selsmarck, and B. J. Sheldon, J. Phys. C **20**, 29 (1987).

¹⁰C. S. G. Cousins, L. Gerward, J. Staun Olsen, B. Selsmark, B. J. Sheldon, and G. E. Webster, Semicond. Sci. Technol. **4**, 333 (1989).

¹¹J. Liu, D. D. Cannon, K. Wada, Y. Ishikawa, D. T. Danielson, S. Jongthammanurak, J. Michel, and L. C. Kimerling, Phys. Rev. B

70, 155309 (2004).

¹²*Semiconductors: Group IV Elements and III-V Compounds*, Landolt-Börnstein, New Series, Group III, Vol. 17, Pt. A, edited by O. Madelung (Springer, Berlin, 1982); *Semiconductors: Intrinsic Properties of Group IV Elements and III-V, II-VI and I-VII Compounds*, Landolt-Börnstein, New Series, Group III, Vol. 22, Pt. A, edited by O. Madelung (Springer, Berlin, 1987).

¹³C. N. Koumelis, G. E. Zardas, C. A. Londos, and D. K. Leventuri, Acta Crystallogr., Sect. A: Cryst. Phys., Diffr., Theor. Gen. Crystallogr. **32**, 84 (1975).

¹⁴L. Brey, N. E. Christensen, and M. Cardona, Phys. Rev. B **36**, 2638 (1987).

¹⁵Z.-Q. Gu, M.-F. Li, J.-Q. Wang, and B.-S. Wang, Phys. Rev. B **41**, 8333 (1990).

¹⁶ δ_{001} , reads as b_d in Ref. 7.

¹⁷I. Balslev, Phys. Rev. **143**, 636 (1966).

¹⁸L. Pedesseau and J. Even (private communication).

¹⁹Y.-H. Li, X. G. Gong, and S.-H. Wei, Phys. Rev. B **73**, 245206 (2006).

²⁰D. Rönnow, N. E. Christensen, and M. Cardona, Phys. Rev. B **59**, 5575 (1999).